Applied Biochemistry and Biotechnology
https://doi.org/10.1007/s12010-026-05712-y

ORIGINAL ARTICLE

In Vitro Evaluation of Novel Synthetic Benzimidazolium–Chalcone Hybrids: Antioxidant and Regenerative Effects in Diabetic Wound Healing

Burcu Demirbağ[1] · Hakan Ünver[2] · Ayça Kara[3] · Adem Necip[4] · Metin Yıldırım[5]

Accepted: 21 April 2026
© The Author(s) 2026

Abstract
The prevalence of diabetes mellitus (DM) is increasing daily worldwide. DM patients suffer from numerous complications, including the development of chronic wounds that can lead to amputation. These complications necessitate innovative approaches. As part of these innovative approaches, this study synthesized four chalcone derivatives and evaluated their activities in an in vitro diabetic wound model. Several spectroscopic techniques, including 1 H and 13 C NMR and HR-MS, were used to confirm the structures of the newly synthesized compounds. After investigating the inhibition of α-glucosidase in HDF-1 cells treated with D-glucose (50 mM), MTT tests and scratch tests were performed. Tumor necrosis factor-alpha (TNF-α), interleukin-1 beta (IL-1β), total antioxidant status (TAS), and procollagen type-1 were analyzed using an ELISA kit. Additionally, proliferation (Ki67), inflammatory (Nuclear factor kappa B; NFκB), and growth factor (Platelet-derived growth factor subunit A; PDGFA) markers in fibroblasts were assessed by immunohistochemistry. All compounds exhibited strong α-glucosidase inhibitory activity, with IC_{50} values ranging from 1.115 to 1.612 μg/mL. Cytotoxicity analysis demonstrated that all compounds were biocompatible, maintaining over 85% cell viability in HDF-1 cells. Under diabetic conditions, treatment significantly improved cell viability and promoted wound closure, particularly in C4. In addition, the compounds reduced pro-inflammatory cytokines TNF-α and IL-1β while increasing TAS and procollagen type I levels. Immunocytochemical findings revealed enhanced Ki67 and PDGFA expression and decreased NFκB activation in treated groups. Molecular docking analysis supported the experimental findings by demonstrating favorable binding interactions with α-glucosidase. In conclusion, chalcone derivatives—particularly compound C4—promote diabetic wound healing through multitarget mechanisms involving anti-inflammatory, antioxidant, and pro-regenerative effects, highlighting their strong therapeutic potential.

Keywords Chalcone · Wound healing · HDF-1 · Diabetes · α-glucosidase

Extended author information available on the last page of the article

Published online: 08 May 2026

Introduction

Diabetes is a metabolic disease characterized by persistently high blood sugar levels. Diabetic wounds, one of the serious complications associated with diabetes, are characterized by chronic inflammation, decreased angiogenesis, dysfunctional fibroblast activity, and impaired tissue repair [1]. In diabetes, hyperglycemia-induced dysfunction of Glucose Transporters (GLUTs) can impair energy-dependent repair functions by reducing glucose uptake in keratinocytes, fibroblasts, and immune cells [2, 3]. High glucose suppresses fibroblast migration and proliferation, impairs tissue repair by reducing collagen synthesis and growth factors, and increases oxidative stress and chronic inflammation [4, 5]. Consequently, wound failure and even foot or lower extremity amputation can occur [6]. Impaired wound healing presents complex challenges that necessitate new therapeutic strategies targeting the interconnected phases of inflammation, proliferation, angiogenesis, and remodeling [6, 7]. These phases are regulated by interactions among keratinocytes, fibroblasts, endothelial cells, inflammatory cells, and a network of bioactive mediators, including extracellular matrix components, growth factors, and cytokines [8, 9]. However, because this process is impaired in diabetic patients, a comprehensive understanding of the precise impact of wounds on individuals with diabetes is crucial to optimizing wound healing outcomes by facilitating the implementation of personalized interventions [10].

Diabetes pathophysiology involves not only hyperglycemia but also oxidative stress, inflammation, and altered cellular signaling. Recent research highlights natural bioactive compounds with multi-targeted effects for diabetes management. For instance, methanolic extracts of *Trigonella foenum-graecum* seeds lower blood glucose and enhance antioxidant defenses in diabetic models [11]. *Bitter melon (Momordica charantia)* seed-enriched foods reduce hyperglycemia and improve metabolic parameters. Lotusine, a lotus alkaloid, mitigates hyperglycemia-induced oxidative stress by modulating the IRS-1/PI3K/Akt pathway [12]. The polyphenolic extract of *Acacia senegal (gum arabic)* also demonstrates antioxidant, antidiabetic, and cytoprotective effects [13]. Moreover, plant-derived compounds, including garlic (Allium sativum) and ginger (Zingiber officinale), have shown promise in diabetes management due to their antioxidant, anti-inflammatory, and metabolism-regulating properties [14, 15]. These findings underscore the importance of metabolic regulation, oxidative stress reduction, and modulation of signaling pathways in minimizing diabetes-related cellular damage. A related study found that a protein-based functional hydrogel significantly accelerated diabetic wound healing by improving the cellular microenvironment, regulating inflammation, enhancing angiogenesis, and promoting cutaneous nerve regeneration [16]. Therefore, strategies that include both nutritional and natural bioactive components and pharmacological approaches are gaining importance in diabetic wound healing. The agents investigated in this study differ from classical chalcone derivatives, as they are benzimidazolium–chalcone hybrid compounds that integrate two pharmacologically active structural motifs, benzimidazole and chalcone, within a single molecule. While the antidiabetic, antioxidant, and anti-inflammatory properties of chalcone derivatives have been extensively documented, research on the effects of these hybrid structures on fibroblast function, especially in the context of diabetic wound healing, remains limited [17, 18].

Although many treatments have been proposed to heal diabetic wounds, a global problem, only a few moderately effective compounds are currently applied clinically [7]. Chalcones are a class of flavonoid precursors with diverse biological activities, includ-

ing anti-inflammatory, antimicrobial, and pro-angiogenic effects, making them promising candidates for diabetic wound healing [14, 19]. Chalcones can suppress hyperglycemia by inhibiting α-glucosidase and α-amylase enzymes [20, 21]. They can reduce insulin resistance by activating peroxisome proliferator-activated receptor gamma (PPARγ) and reduce inflammation by inhibiting NFκB and cyclooxygenase-2 (COX-2) pathways [20]. In addition, they can increase the expression of antioxidant enzymes (Superoxide Dismutase (SOD), Catalase (CAT), Glutathione Peroxidase (GPx)) by activating the Nuclear factor erythroid 2–related factor 2 (Nrf2)/Antioxidant Response Element (ARE) pathway [22, 23]. It can exhibit strong antioxidant properties thanks to its ability to scavenge free radicals [24]. With these properties, various chalcone derivatives (methochalcone and sochalcone) have been approved as bile expectorant drugs and antiulcer agents, respectively, and have been reported to alleviate symptoms in clinical studies for chronic venous lymphatic insufficiency [25]. These natural compounds have several advantages: availability, ease of application, safe pharmacology, high efficacy, and affordable price [8]. In addition, chalcones are more stable and can be converted into promising bioactive scaffolds in medicinal chemistry [26]. Preclinical studies show that chalcones may be effective in treating diabetes and its complications through multiple mechanisms of action [17, 27]. A study reported that chalcone derivatives, 4-hydroxyderricin and xanthoangelol, significantly enhanced wound healing, particularly in endothelial cells. Another study suggested that chalcone, when combined with berberine, reduces oxidative stress and inflammation, increasing cell regeneration and thus promoting faster wound healing. Our study examined the therapeutic effects of newly synthesized chalcones on a glucose-induced in vitro wound model of diabetic fibroblasts, via multiple mechanisms.

Materials & Methods

All reagents and solvents were obtained from commercial suppliers and used without further purification. NMR spectra were acquired on an Agilent 400 MHz FT-NMR spectrometer. High-resolution mass spectrometry (HRMS) was performed using an Agilent 6545 Accurate-Mass QTOF-MS instrument to determine the molecular masses. Reaction progress was monitored by thin-layer chromatography (TLC) on silica gel plates.

Synthesis Procedure of Compound 1 (3-(4-(1 H-benzo[d]imidazol-1-yl)phenyl)−1-phenylprop-2-en-1-one)

A solution of potassium hydroxide (1.5 equiv.) in ethanol was added dropwise to an ethanolic solution containing equimolar amounts of 4-(1 H-benzo[d]imidazol-1-yl)benzaldehyde and acetophenone at room temperature. The reaction mixture was stirred for 12 h, during which a solid gradually precipitated. The resulting solid was isolated by filtration, washed with a 1:5 ethanol/water mixture, dried, and used in subsequent steps without further purification (yield: 83%) [28].

^{1}H-NMR (400 MHz, DMSO-d^6) δ (ppm): 8.64 (s, 1 H, Benzimidazole CH), 8.17 (dd, J=11.1, 8.4 Hz, 4 H), 8.04 (d, J=15.6 Hz, 1 H, CH=CH), 7.84 (d, J=15.6 Hz, 1 H, CH=CH), 7.79 (dd, J=7.8, 3.1 Hz, 3 H, Ar-H), 7.73–7.64 (m, 2 H, Ar-H), 7.59 (t, J=7.6 Hz, 2 H, Ar-H), 7.34 (pd, J=7.2, 1.4 Hz, 2 H, Ar-H). **^{13}C-NMR (100 MHz, DMSO-d^6) δ**

(ppm): 189.62, 144.42, 143.70, 143.26, 137.99, 137.98, 134.34, 133.72, 133.21, 131.07, 129.30, 129.05, 124.16, 124.13, 123.81, 123.20, 123.16, 120.52, 111.36, 39.98.

Synthesis Procedure of Benzimidazolium-Chalcone Hybrid Compounds

Four separate reactions were performed to synthesize each target compound. For each reaction, 100 mg (0.3 mmol) of Compound 1 was weighed into a 50 mL round-bottom flask and dissolved in 10 mL of acetonitrile (CH_3CN) at 70 °C using a magnetic stirrer-heater. Subsequently, 0.3 mmol of the corresponding reagents—2-bromo-1-(4-nitrophenyl)ethan-1-one (2a), 2-bromo-1-(4-bromophenyl)ethan-1-one (2b), 2-bromo-1-(4-(trifluoromethyl) phenyl)ethan-1-one (2c), and 2-bromo-1-(naphthalen-2-yl)ethan-1-one (2d)—were added individually to the respective flasks. The reaction mixtures were stirred at 70 °C for 48 h. Upon completion of the reactions, as monitored by Thin Layer Chromatography (TLC), the solutions were allowed to cool to room temperature. The resulting precipitates were washed twice with diethyl ether, collected by centrifugation, and dried under vacuum to afford the pure products as C1-C4. All target molecules remained stable under ambient conditions and direct air exposure for a period of four months.

3-(2-(4-nitrophenyl)−2-oxoethyl)−1-(4-(3-oxo-3-phenylprop-1-en-1-yl)phenyl)−1 H-benzo[d]imidazol-3-ium bromide (C1)

Yield: 85%. **^{1}H-NMR (400 MHz, DMSO-d^6) δ (ppm)**: 10.15 (s, 1 H, Benzimidazolium CH), 8.49 (d, J=8.3 Hz, 2 H, Ar-H), 8.40 (d, J=8.3 Hz, 2 H, Ar-H), 8.30 (d, J=8.2 Hz, 2 H, Ar-H), 8.21 (t, J=6.9 Hz, 3 H, Ar-H), 8.15 (d, J=15.6 Hz, 1 H, CH=CH), 7.98 (t, J=9.3 Hz, 3 H, Ar-H), 7.89 (d, J=15.6 Hz, 1 H, CH=CH), 7.82–7.74 (m, 2 H), 7.70 (t, J=7.1 Hz, 1 H, Ar-H), 7.60 (t, J=7.5 Hz, 2 H, Ar-H), 6.57 (s, 2 H, ethylene -CH_2-). **^{13}C-NMR (100 MHz, DMSO-d^6) δ (ppm)**: 190.69, 189.58, 151.17, 144.03, 142.45, 138.80, 137.78, 137.36, 134.60, 133.92, 132.43, 131.18, 131.09, 130.45, 129.35, 129.13, 128.16, 127.81, 126.09, 124.80, 124.60, 115.01, 114.24, 54.35. **HRMS (m/z)** $[M\text{-}Br]^+$: calcd for $C_{30}H_{22}N_3O_4^+$: 488.5225; found: 488.3038.

3-(2-(4-bromophenyl)−2-oxoethyl)−1-(4-(3-oxo-3-phenylprop-1-en-1-yl)phenyl)−1 H-benzo[d]imidazol-3-ium bromide (C2)

Yield: 75%. **^{1}H-NMR (400 MHz, DMSO-d^6) δ (ppm)**: 10.14 (s, 1 H, Benzimidazolium CH), 8.29 (d, J=8.4 Hz, 2 H, Ar-H), 8.22–8.14 (m, 3 H, Ar-H including CH=CH bond), 8.13–8.06 (m, 3 H, Ar-H), 7.97 (t, J=9.3 Hz, 3 H, Ar-H), 7.93–7.84 (m, 3 H, Ar-H including CH=CH bond), 7.79–7.72 (m, 2 H, Ar-H), 7.69 (t, J=7.3 Hz, 1 H, Ar-H), 7.59 (t, J=7.5 Hz, 2 H, Ar-H), 6.47 (s, 2 H, ethylene -CH_2-). **^{13}C-NMR (100 MHz, DMSO-d^6) δ (ppm)**: 190.67, 189.59, 144.06, 142.45, 137.79, 137.34, 134.62, 133.92, 133.21, 132.70, 132.45, 131.19, 131.07, 130.92, 129.36, 129.14, 128.13, 127.81, 126.06, 124.80, 114.94, 114.23, 53.89. **HRMS (m/z)** $[M\text{-}Br]^+$: calcd for $C_{30}H_{22}BrN_2O_2^+$: 522.4215; found: 523.2270.

3-(2-oxo-2-(4-(trifluoromethyl)phenyl)ethyl)−1-(4-(3-oxo-3-phenylprop-1-en-1-yl) phenyl)−1 H-benzo[d]imidazol-3-ium bromide (C3)

Yield: 74%. **^{1}H-NMR (400 MHz, DMSO-*d*^{6}) *δ* (ppm)**: 10.21 (s, 1 H, Benzimidazolium CH), 8.37 (d, *J* = 7.9 Hz, 2 H, Ar-H), 8.31 (d, *J* = 8.0 Hz, 2 H, Ar-H), 8.20 (d, *J* = 7.7 Hz, 3 H, Ar-H), 8.15 (d, *J* = 15.6 Hz, 1 H, CH = CH), 8.07 (d, *J* = 8.0 Hz, 2 H, Ar-H), 7.99 (dd, *J* = 11.7, 8.4 Hz, 3 H, Ar-H), 7.89 (d, *J* = 15.6 Hz, 1 H, CH = CH), 7.82–7.73 (m, 2 H, Ar-H), 7.70 (t, *J* = 7.3 Hz, 1 H), 7.60 (t, *J* = 7.4 Hz, 2 H, Ar-H), 6.58 (s, 2 H, ethylene -CH_2-). **^{13}C-NMR (100 MHz, DMSO-*d*^{6}) *δ* (ppm)**:190.96, 189.59, 144.06, 142.46, 137.79, 137.44, 137.36, 134.63, 134.29, 133.97, 133.92, 132.46, 131.20, 131.08, 129.88, 129.36, 129.15, 128.15, 127.82, 126.57, 126.53, 126.08, 125.49, 124.81, 122.78, 115.01, 114.25, 54.27. **HRMS (m/z)** $[M\text{-}Br]^+$: calcd for $C_{31}H_{22}F_3N_2O_2^+$: 511.5237; found: 511.3077.

3-(2-(naphthalen-2-yl)−2-oxoethyl)−1-(4-(3-oxo-3-phenylprop-1-en-1-yl)phenyl)−1 H-benzo[d]imidazol-3-ium bromide (C4)

Yield: 78%. **^{1}H-NMR (400 MHz, DMSO-*d*^{6}) *δ* (ppm)**: 10.26 (s, 1 H, Benzimidazolium CH), 9.00 (s, 1 H, Ar-H), 8.33 (d, *J* = 8.1 Hz, 2 H, Ar-H), 8.21 (ddd, *J* = 20.5, 14.4, 7.7 Hz, 6 H, Ar-H including CH = CH bond), 8.10 (dd, *J* = 8.2, 4.8 Hz, 2 H, Ar-H), 8.01 (dd, *J* = 13.3, 5.7 Hz, 3 H, Ar-H), 7.90 (d, *J* = 15.7 Hz, 1 H, CH = CH), 7.75 (ddt, *J* = 24.4, 13.3, 6.0 Hz, 5 H, Ar-H), 7.61 (t, *J* = 7.6 Hz, 2 H, Ar-H), 6.66 (s, 2 H, ethylene -CH_2-). **^{13}C-NMR (100 MHz, DMSO-*d*^{6}) *δ* (ppm)**: 191.19, 189.56, 144.15, 142.51, 137.76, 137.30, 136.10, 134.69, 133.96, 132.55, 132.52, 131.57, 131.43, 131.23, 131.07, 130.23, 129.97, 129.38, 129.28, 129.16, 128.42, 128.13, 127.97, 127.83, 126.06, 124.70, 123.81, 114.96, 114.27, 53.98. **HRMS (m/z)** $[M\text{-}Br]^+$: calcd for $C_{34}H_{25}N_2O_2^+$: 493.5855; found: 493.3280.

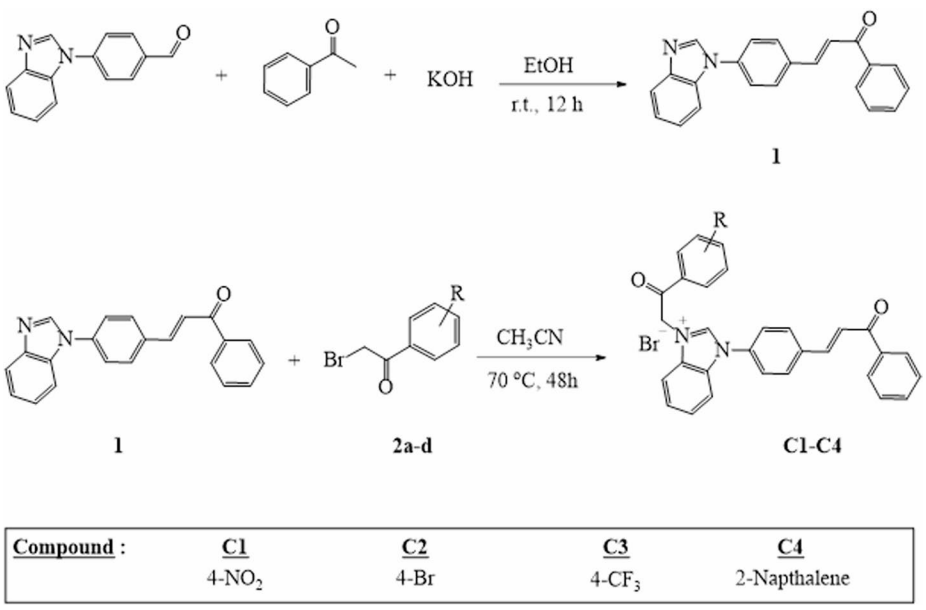
The synthesis scheme of benzimidazolium-chalcone hybrid compounds is given in Fig. 1.

Cell Culture and Experimental Groups

The human dermal fibroblast cell line (HDF-1), a crucial component of our experiments, was purchased from Atlas Biotechnology. HDFs were maintained in Dulbecco's Modified Eagle Medium (DMEM) (Wisent Inc. 319-013-CL) supplemented with 10% fetal bovine serum (FBS), 2% L-glutamine, and 1% penicillin-streptomycin (Gibco). For the diabetic group, cells were incubated with D-glucose (Merck) (50 mM) for 72 h [29, 30].

α-Glucosidase Activity Assay

The α-glucosidase inhibitory activity was evaluated according to our previously reported method. The inhibitory potentials of compounds bearing different substituents were assessed at concentrations ranging from 0.5 to 2 µg/mL. Briefly, test samples at various concentrations were added to the enzyme solution prepared in phosphate buffer. Following incubation, the substrate α-D-glucopyranoside was introduced, and absorbance was measured at 405 nm using a spectrophotometer. Each experiment was performed in triplicate. Acarbose was used as positive control [31].



Compound :	C1	C2	C3	C4
	4-NO_2	4-Br	4-CF_3	2-Napthalene

Fig. 1 Synthesis procedure of benzimidazoium-chalcone hybrid derivatives

3-(4,5-Dimethylthiazol-2-yl)−2,5 – 2,5-Diphenyltetrazolium Bromide (MTT) Assay

The MTT assay, a well-established protocol, uses a tetrazolium salt that is reduced by mitochondrial metabolism in living cells, forming a purple formazan product. The MTT kit (Cayman) was used to evaluate the toxicity of chalcone compounds. HDF-1 cells were seeded at a density of 2.5×10^4 cells/well in a 96-well plate and incubated overnight. After 24 h, cells were treated with chalcone (1 µM, 5 µM, 25 µM, 50 µM, 100 µM) compounds for 24 h. After the indicated time points, the culture medium was removed for the MTT assay, and 20 µL of MTT solution (5 µg/mL) was added to each well. The plates were then incubated at 37 °C for 4 h, and after removing the MTT solution, 100 µL of DMSO (Sigma) was added to dissolve formazan crystals. Absorbance was measured at 570 nm using a microplate reader (Thermo Scientific Multiskan Go) [8].

Wound Scratch Assay

High-glucose environments are a standard approach for simulating diabetes in in vitro studies and are widely used to mimic a diabetic environment. Therefore, in our study, a diabetic wound model was created using 50 mM D-glucose for 72 h [4]. HDF-1 cells were seeded in a 12-well plate. Then, the IC_{50} values of all compounds were determined in diabetic HDF-1 cells. After 48 h, a "scratch" was created with a 200-µL pipette tip. Fibroblast migration was photographed at 0, 24, and 48 h using an inverted microscope equipped with a digital camera (Euromex) to ensure data accuracy. The ImageJ software was used to measure the scratch area [32]. Wound closure percentage was calculated based on the initial wound area and the wound area at a specific time point: 24 h wound healing rate = (0 h distance-24 h

distance)/0 h distance × 100, and 48 h wound healing rate = (0 h distance-48 h distance)/0 h distance × 100.

Total Antioxidant Status (TAS) Measurement

Adhering strictly to the manufacturer's instructions, we determined TAS levels in HDF-1 cells using the TAS Colorimetric Assay Kit (Elabscience, E-BC-K801-M). Trolox was prepared at different concentrations as a positive control and used as a reference standard for TAS measurements. The TAS values in our samples were then calculated as mmol/L, ensuring the validity of our Method [14].

Type I Procollagen and Cytokine Analysis

Type I procollagen (BTB-E1385Hu), TNF-α (BT Lab, E0082Hu), and IL-1β (BT Lab, E0119Ra) levels were quantified using an enzyme-linked immunosorbent assay (ELISA). The analysis was performed according to the instructions provided with the kits. The absorbance of all groups was measured at 450 nm using a microplate reader (Thermo Scientific Multiskan Go) [33].

Ki67, NFκB, PDGFA Immunostain

HDF-1 cells grown on coverslips were fixed with 4% paraformaldehyde, permeabilized with 0.1% Triton X-100, and endogenous peroxidase activity was blocked using 3% H_2O_2. After blocking, cells were incubated overnight at 4 °C with Ki67 (bs-2310R), NFκB (bs-10037R), and PDGFA (bs-0196R) primary antibodies (Bioss Antibodies), followed by HRP-conjugated secondary antibodies. Immunoreactivity was visualized using DAB and counterstained with hematoxylin [34, 35]. Immunoreactivity was assessed semi-quantitatively using the H-score system, which incorporates both staining intensity and the percentage of positive cells. The staining intensity (scored 0 to 3) was multiplied by the proportion of positive cells (scored 0 to 4) to yield a total score ranging from 0 to 12 [36].

Molecular Docking

Molecular docking was performed using Maestro (version 13.8). The chemical structures of the synthesized compounds were prepared using ChemDraw. The three-dimensional structure of the α-glucosidase–related protein (PDB ID: 5NN8) was obtained from the Protein Data Bank. After protein preparation, a receptor grid box with dimensions of 20 × 20 × 20 Å was generated to define the active site. Docking results were evaluated and expressed as binding energies (kcal/mol) [14, 37–39].

Statistical Analysis

Experimental data are reported as mean ± standard deviation (SD) from three independent experiments ($n = 3$). One-way ANOVA assessed differences between groups for each biological endpoint. Post hoc tests compared treatment groups with the diabetic group, with significance set at $p < 0.05$. For direct comparisons between treatment groups, pairwise anal-

yses used Bonferroni post hoc tests, depending on normality and homogeneity of variance. All statistical analyses and graphs were produced using GraphPad Prism 9.0 (GraphPad Software, San Diego, CA, USA).

Result

Chemistry

The synthetic routes for Compound 1 and the benzimidazolium–chalcone hybrid derivatives are illustrated in Fig. 1. Compound 1 was obtained by reacting the corresponding aldehyde and acetophenone at room temperature for 30 min. Compound 1 was dissolved in acetonitrile to prepare the quaternary ammonium salts and reacted with the appropriate benzyl bromide derivatives. Four novel products were isolated as pure precipitates. The structures of all synthesized compounds were confirmed by ^{1}H and ^{13}C NMR spectra, acquired on an Agilent 400 MHz FT-NMR spectrometer. Additionally, high-resolution mass spectrometry (HRMS) was performed using an Agilent 6545 Accurate-Mass QTOF-MS instrument to determine the molecular masses.

Spectroscopic Analysis of the Compounds

The ^{1}H NMR spectrum of Compound 1 (Fig. S1) exhibited a singlet at 8.64 ppm, attributed to the benzimidazole CH proton. The aromatic and other proton resonances were observed within the expected chemical shift range of 7.31–8.19 ppm. In addition, the conjugated alkene fragment should exhibit characteristic signals in the 1 H NMR spectrum. The corresponding protons are expected to appear as doublets with a coupling constant of approximately $J \approx 16$ Hz (consistent with a trans-configuration). The ^{1}H NMR spectra of the benzimidazolium–chalcone derivatives (C1–C4) (Supplement file) (Figs. S3, S6, S9, S12) displayed singlet signals near 6.5 ppm, corresponding to the methylene (–CH_2–) protons, with each signal integrating for two protons. For all derivatives, aromatic and olefinic (–CH=CH–) proton signals were observed in the range of 7.57–8.50 ppm. The benzimidazolium CH proton appeared as a distinct resonance around 10 ppm.

In the ^{13}C NMR spectrum of Compound 1 (Fig. S2), the carbonyl (C=O) carbon appeared at 189.62 ppm, while aromatic carbons resonated between 111.36 and 144.42 ppm. In the ^{13}C NMR spectra of the benzimidazolium–chalcone hybrid salts (C1-C4), signals appearing near 50 ppm were assigned to the methylene (–CH_2–) carbons (Figs. S4, S7, S10, S13). Aromatic and olefinic carbon resonances were observed across the range of 114.23–151.17 ppm for all compounds. The carbonyl (C=O) carbons adjacent to the –CH=CH– moiety appeared around 189 ppm, while additional carbonyl signals, associated with the benzimidazole ring, were detected near 190 ppm in each compound.

In addition, high-resolution mass spectrometry (HRMS) analysis of all compounds was consistent with the calculated molecular masses (Figs. S5, S8, S11, S14).

The comprehensive spectroscopic data conclusively confirm the successful synthesis of the target compounds.

Table 1 IC_{50} values of C1, C2, C3 and C4 against α-Glucosidase

Compounds	Regression equation	R^2	IC_{50} (μg/mL)
C1	y = −0.2788x + 0.8792	0.9859	1.557
C2	y = −0.3578x + 0.8586	0.9914	1.156
C3	y = −0.2544x + 0.8552	0.9554	1.612
C4	y = −0.356x + 0.842	0.98	1.115
Acarbose	y = −0.13x + 0.9004	0.9897	3.503

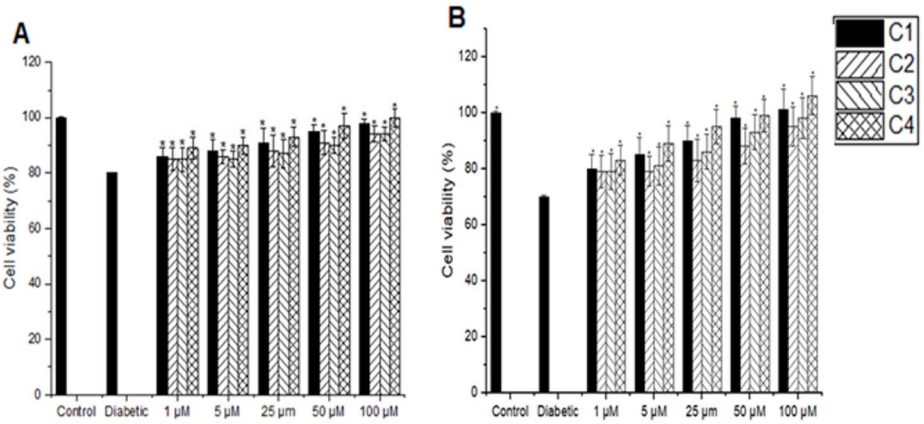


Fig. 2 Diabetic HDF-1 cell viability graph treated with compounds C1, C2, C3, and C4 for 24 (**A**) and 48 h (**B**). Control: D-glucose and compounds were not added. All values are shown as the mean ± SD of 3 independent experiments ($n = 3$). *When the groups were compared with the diabetic group, $p < 0.05$

α-Glucosidase Activity Assay

The α-glucosidase inhibitory potentials of the compounds prepared at different concentrations were investigated. According to the results, the IC_{50} values ranged from 1.115 to 1.557 μg/mL. Among the tested compounds, compound C4 exhibited the strongest inhibitory activity. Acarbose was used as the positive control, and its IC_{50} value was calculated as 3.503 μg/mL (Table 1). These findings demonstrate that the synthesized compounds act as more potent α-glucosidase inhibitors than the positive control.

Cell Viability

Compounds applied to HDF-1 cells at concentrations of 1 μM (C1, C2, C3, C4: 86.3 ± 3.1, 85.3 ± 4.2, 85 ± 5.3, 89.6 ± 6.1 respectively), 5 μM (88 ± 6.2, 86.2 ± 2.5, 85.9 ± 2.8, 90.2 ± 3.1 respectively), 25 μM (91.2 ± 5.3, 88.4 ± 6.7, 87.1 ± 8.2, 93.2 ± 3.4 respectively), 50 μM (95.7 ± 2.3, 91.4 ± 3.1, 90.5 ± 2.8, 97.6 ± 4.4 respectively), and 100 μM (98.6 ± 2.5, 94.4 ± 2.9,94.1 ± 2.5, 99.7 ± 3.5 respectively), did not reduce cell viability (%) at 24 h compared to the control group (100 ± 0.3) (Fig. 2A). At the end of 24 h of incubation, HDF-1 cells treated with various concentrations of C1 and C4 (50–100 μM) were similar to the control group (Fig. 2A) ($p > 0.05$). Also, HDF-1 cells treated with C2 and C3 showed similar cell viability (Fig. 2A) ($p > 0.05$). In the MTT assay, HDF-1s treated with compounds C1, C2, C3, and C4 at 48 h (1 μM: 80.2 ± 5.9, 79.5 ± 5.7, 79.3 ± 6.3, 83.7 ± 5.2, 5 μM: 85.4 ± 6.1,

81.8 ± 5.4, 79.5 ± 6.8, 89.6 ± 6.4, 25 µM: 90.1 ± 5.3, 86.5 ± 7.6, 83.6 ± 6.2, 95.2 ± 6.1, 50 µM: 98.4 ± 4.3, 93.4 ± 6.2, 88.2 ± 6.1, 99.1 ± 6.5, 100 µM: 101.2 ± 7.5, 98.5 ± 6.9, 95.7 ± 7.3, 106.1 ± 6.8 respectively) of incubation showed increased cell viability (%), compared to the diabetic group (70.3 ± 0.9) (Fig. 2A and B) ($p < 0.05$). In diabetic HDF-1 cells, after 48 h of incubation, all compounds had approximately 80% viable cells at the lowest experimental concentration 1–5 µM (Fig. 2B) ($p < 0.05$). This indicates that the compounds exhibit a remarkably nontoxic.

Migration Assay

In the scratch analysis, there was a wound healing percentage of 48.8% in the control group at 24 h, while all treatment groups (49.3 ± 1.5, 48.2 ± 1.6, 47.7 ± 1.9, and 50.4 ± 2.1 respectively) were similar to the control group (48.1 ± 1.1) (Fig. 3B) ($p > 0.05$). There was a wound healing percentage of 89.7 ± 2.3 in the control group at 48 h, while compounds C1 and C4 (87.2 ± 2.8 and 90.3 ± 2.1 respectively) were similar to the control group (Fig. 3A) ($p > 0.05$). However, as shown in Fig. 3, the wound-healing percentages of groups C2 and C3 at 48 h (58.6 ± 3.1 and 66.2 ± 2.8 respectively) were lower than those of the control group ($p < 0.05$). The diabetic group exhibited wound-healing percentages of 49.4 ± 2.6 at 48 h, which were significantly lower than those of all treatment groups (Fig. 3B) ($p < 0.05$).

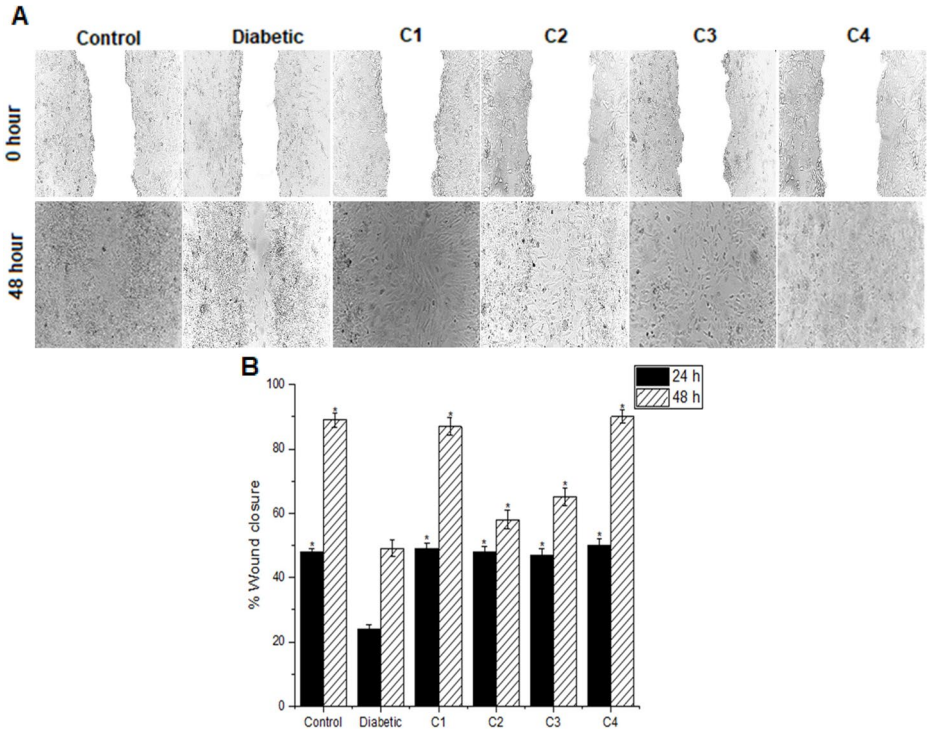


Fig. 3 Microscopic image of diabetic HDF-1 cell migration (**A**) and % wound closure rate (**B**) treatment with C1, C2, C3, and C4. All values are shown as the mean±SD of 3 independent experiments (n = 3). *When the groups were compared with the diabetic group, p<0.05

TNF-α, IL-1β, Procollagen Type I, and TAS Levels

TNF-α and IL-1β levels were 227.2±2.2 and 979.2±7.3 respectively, in the control group. Following chalcone treatment of HDF-1 cells treated with D-glucose, C4, in particular, reduced TNF-α (C1, C2, C3, C4: 322.1±7.2, 358.6±6.1, 285.4±5.3, 273.7±6.8 respectively) and IL-1β (C1, C2, C3, C4: 1236.3±16.6, 1335.2±15.3, 1233.4±18.3, 1118.2±19.3 respectively) levels compared to the diabetic group (TNF-α: 442.4±5.3, IL-1β: 1642.4±8.6) (Fig. 4A and B) ($p<0.05$). Glucose disrupts the oxidative balance in HDF-1 cells, as evidenced by a decreased antioxidant capacity (Fig. 4C) ($p<0.05$). However, after treatment with all compounds, TAS (C1, C2, C3, C4:1.35±0.12, 1.15±0.10, 1.18±0.11, 1.5±0.15 respectively) and procollagen type I (C1, C2, C3, C4: 79.2±1.9, 70±2.3, 79.4±2.6, 88.3±2.1 respectively) levels in HDF-1 cells were observed to increase compared to the diabetic group (TAS: 0.6±0.10, procollagen type I: 63.1±0.8) (Fig. 4C and D) ($p<0.05$). Additionally, TAS levels in diabetic cells treated with C1 and C4 were higher than in the control group (1.04±0.09) (Fig. 4C) ($p<0.05$). On the other hand, type I procollagen levels

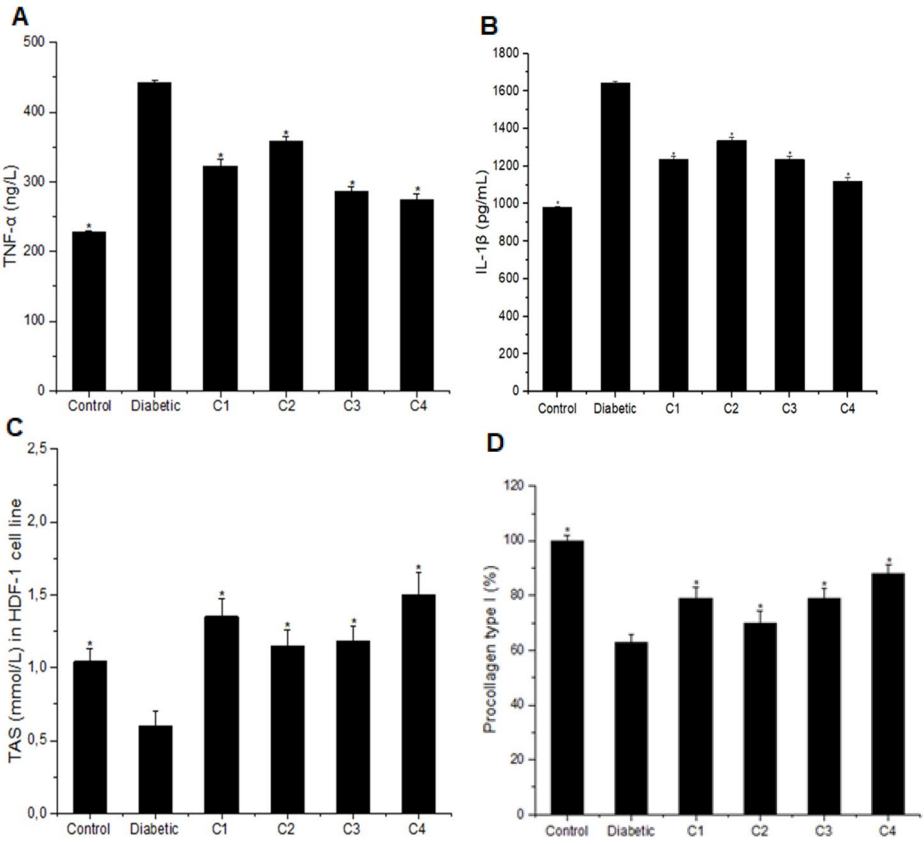


Fig. 4 Comparative graphs showing the TNF-α (**A**), IL-1β (**B**), TAS (**C**), and procollagen type I levels (**D**) in diabetic HDF-1 cells treated with C1, C2, C3, and C4. All valuesare shown as the mean±SD of 3 independent experiments (n = 3). *When the groups were compared with the diabetic group, p<0.05

in treated diabetic HDF-1 cells were lower than in the control group (100.2 ± 0.9) (Fig. 4D) ($p < 0.05$).

Immunolabeling of Ki67, NFκB, PDGFA

According to the H-score evaluation, the treatment groups showed a statistically significant increase in Ki67 nuclear and PDGFA cytoplasmic immunoreactivity compared to the diabetic group ($p < 0.05$) (Fig. 5A and B, and 5D). In contrast, NFκB nuclear immunoreactivity H-scores were significantly decreased in the treatment groups relative to the diabetic group ($p < 0.05$) (Fig. 5A and C). These results indicate that compounds C1, C2, C3, and C4 may suppress NFκB activity while enhancing cellular proliferation and growth factor expression.

Molecular Docking

Among the synthesized compounds, compound C4 exhibited the strongest α-glucosidase inhibitory activity and was therefore selected for molecular docking analysis to investigate its interaction with the 5NN8 α-glucosidase protein. According to the docking results, compound 2098 showed a binding energy of −5.051 kcal/mol. Although experimental data

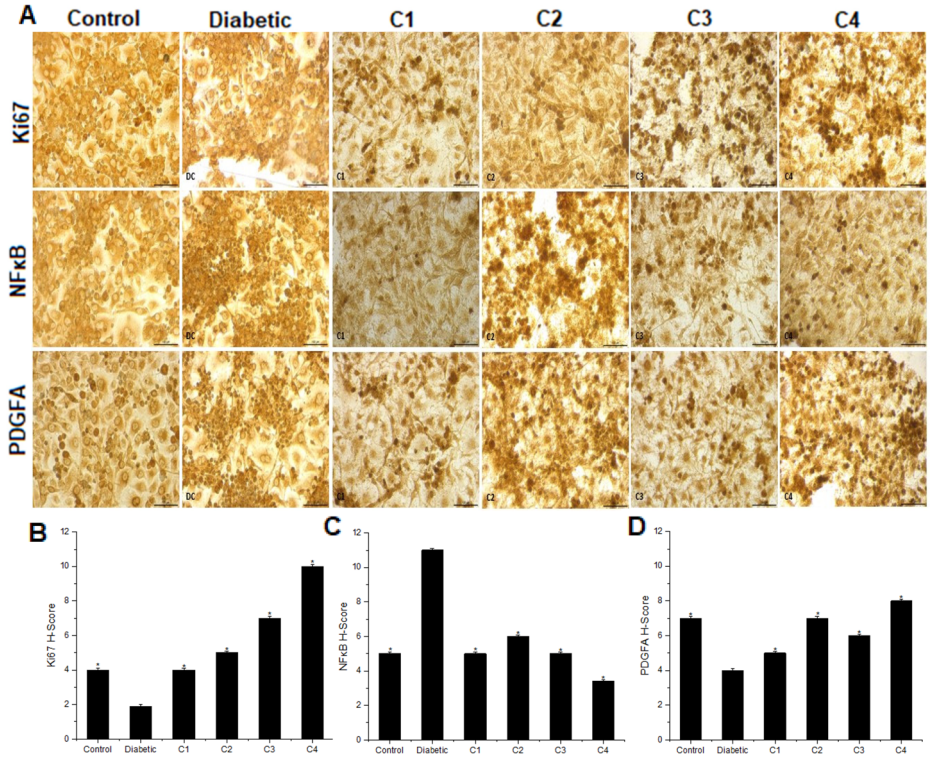


Fig. 5 Representative histological image of diabetic HDF-1 cells following treatment with C1, C2, C3, and C4, and subsequent immunostaining for Ki67, NFκB, and PDGFA. Scale bars: 100 µm (**A**). H-score graph of Ki67 (**B**), NFκB (**C**), and PDGFA (**D**) immunoreactivity (mean±SD). *When the groups were compared with the diabetic group, $p<0.05$

Table 2 Molecular docking scores and Glide emodel values

Compounds	Protein	Docking score	Glide e model
C4	5NN8	−5.051	−63.330
Acarbose	5NN8	−7.168	−92.530

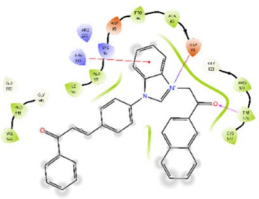
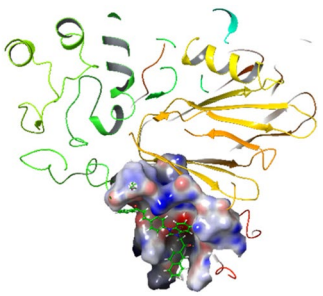
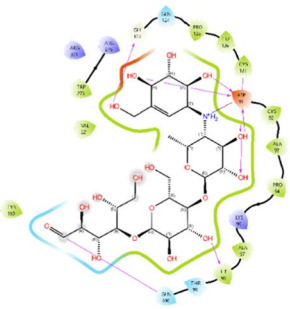
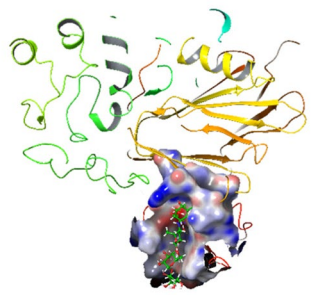
Compounds	**Protein**	**2D**	**3D**
C4	**5NN8**		
Acarbose	**5NN8**		

Fig. 6 2D and 3D structural representations of the target proteins

indicated that compound 2098 was more potent than the positive control acarbose, the docking score of acarbose was calculated as − 7.168 kcal/mol (Table 2).

Interaction analysis revealed that the benzene ring of the benzimidazole moiety forms a π–cation interaction with ARG331. Additionally, the carbonyl group in the structure forms a hydrogen bond with TRP126, while the positively charged nitrogen (N^+) participates in a salt bridge interaction with ASP91. These interactions stabilize compound 2098 within the enzyme's active site (Fig. 6).

Discussion

Wounds in diabetic patients are the leading cause of non-traumatic amputations, with infection accounting for an average mortality rate of 50% [6]. Effective modulation of wound healing is therefore essential. This process includes hemostasis, inflammation, debridement, proliferation, epithelialization, and remodeling [40, 41], but its molecular and cellular regulation remains incompletely understood. Chronic wounds present a major global healthcare challenge and result in significant medical costs [8]. As a result, new strategies to accelerate wound healing are being explored. Chalcones have demonstrated antidiabetic properties

in several studies. They may reduce insulin resistance by regulating adipogenesis via peroxisome proliferator-activated receptor gamma (PPAR-γ) [17], enhance glucose uptake by increasing GLUT4 expression in muscle and adipose tissue, and protect pancreatic β-cells by reducing oxidative stress and chronic inflammation associated with diabetes pathogenesis [17, 42]. This study investigates the effects of newly synthesized chalcones on wound healing in HDF-1 cells under high-glucose conditions, focusing on inflammation, growth factor signaling, antioxidant mechanisms, and cell proliferation.

Chalcones (1,3-diaryl-2-propen-1-ones), as biosynthetic precursors of flavonoids, stand out for their potent antidiabetic properties [43]. These compounds may accelerate healing by increasing fibroblast proliferation in diabetic wound models. One study suggested that various chalcone derivatives increase fibroblast proliferation in vitro and in vivo [44]. Our study confirms increased growth rates in diabetic fibroblasts treated with C1, C2, C3, and C4 compared with untreated diabetic fibroblasts, as observed by Salehi et al. (Figure 2A and B) ($p < 0.05$) [17]. Diabetic wound fibroblasts are likely impaired due to cell senescence associated with or induced by diabetes (intrinsic senescence) and the wound environment [45]. Given that glucose inhibits microtubule formation at high concentrations, we believe that a defect in microtubule structure, which is effective in cell proliferation, may contribute to the intrinsic mechanism involved in the decreased cell proliferation observed in diabetic wound fibroblasts [14, 46]. Therefore, the increased intensity of Ki67 proliferation marker and growth factor immunostaining in the treatment groups compared to the diabetic group, and the correlation of this increase with fibroblast proliferation, support the potential effectiveness of chalcone compounds in this process. Furthermore, effective compound doses were determined using alpha-glucosidase inhibition results. At these concentrations, fibroblast metabolic activity remained stable, while cell proliferation increased. These results demonstrate the compounds' non-toxicity and support their potential for therapeutic application.

Dermal fibroblasts (DF) play a key role in wound healing by proliferating and migrating into the wound bed to form granulation tissue [47]. Previous studies in mice have indicated that the migratory ability of diabetic DFs is impaired, with diabetic DFs migrating 75% less than normal DFs. Recently, a novel naphthalcone derivative, 2-(5-(2,4,6-trimethoxyphenyl)−4,5-dihydro-1 H-pyrazol-3-yl)naphthalen-1-ol (TDPN), demonstrated significant activity in promoting the migration and proliferation of HaCaT cells [48]. In this study, glucose inhibited DF migration, but chalcone compounds reversed this effect (Fig. 3 A and B) ($p < 0.05$). Compound C4, which contains a 2-naphthalene ring, demonstrated significantly greater biological activity than chalcones with 4-NO_2, 4-Br, or 4-CF_3 groups (Figs. 1 and 3 A and B) ($p < 0.05$). This enhanced activity was consistent across cell migration and proliferation analyses. Chalcone derivatives with a 2-naphthalene ring are known for high lipophilicity, increased membrane permeability, and strong hydrophobic and π–π interactions with intracellular signaling proteins which likely contribute to C4's superior activity. These features also support more efficient activation of signaling pathways involved in cytoskeletal remodeling and cell cycle progression, accelerating migration and proliferation [49, 50]. These properties are associated with C4's enhanced biological activity. Additionally, these characteristics facilitate more efficient activation of signaling pathways involved in cytoskeletal remodeling and cell cycle progression, thereby accelerating cell migration and increasing proliferation. Other studies have reported that different chalcone derivatives substantially affect the cell cycle and migration of human breast and lung cancer cells, suggesting that the effects of chalcone derivatives on cell migration may vary with structural properties,

concentration, and cell type [51]. In another study, the potent antioxidant properties of chalcone compounds were associated with increased fibroblast cell migration [52]. Chalcone compounds may reduce cell damage by scavenging free radicals and regulate fibroblast proliferation and migration by affecting the cell cycle. On the other hand, cell migration is regulated by various signaling pathways, including MAPK and NFκB [48]. High glucose (hyperglycemia) causes oxidative stress and chronic activation of the NFκB pathway in fibroblast cells, and increases IL-1β production [53]. Consequently, fibroblast migration and proliferation are reduced, and wound healing is delayed or suppressed. Indeed, in our study, the decrease in NFκB immunostaining intensity and TNF-α, IL-1β levels, but an increase in TAS, in the treatment groups compared to the diabetic group, indicates inhibition of the NF-κB pathway by chalcone compounds (Fig. 4A and B, 4 C, and Fig. 5A and C) ($p < 0.05$). This inhibition is significant because it suggests that chalcone compounds may counteract the adverse effects of hyperglycemia on the NFκB pathway, thereby promoting fibroblast migration and wound healing. Furthermore, it was concluded that PDGFA activation modulated cell migration by suppressing NFκB. Indeed, a higher PDGFA H-score was observed in the treatment groups compared to the diabetic group (Fig. 5A and C) ($p < 0.05$). (Figure 5A and C) ($p < 0.05$).

During the inflammatory phase of wound healing, DF secrete cytokines, chemokines, and growth factors that coordinate immune cell migration and support cell survival in damaged tissue [54]. PDGFA is essential for stimulating fibroblast chemotaxis and proliferation [55, 56]. In diabetes, elevated NFκB and IL-1β levels impair PDGFA and TGF-β activation, reducing fibroblast migration [57]. The chalcone treatment in this study shows promise by inducing PDGFA expression, which may enhance fibroblast migration through improved growth factor signaling. This effect is associated with reduced inflammation and increased antioxidant activity, mediated by α-glucosidase inhibition. The reactivation of these growth factors suggests that the compounds lower intracellular oxidative stress through their antioxidant properties. Structural analogs of flavones have been shown to promote procollagen production in DF and provide anti-aging effects [14, 48]. In this study, higher PDGFA levels in the treatment groups directly correlated with increased type I procollagen production, the main structural protein in new connective tissue (Figs. 4D and 5A and D) ($p < 0.05$). The results indicate that the biological activity of chalcone derivatives depends on both their core scaffolds and substituents. Compound C4, which contains a 2-naphthalene ring, showed greater activity than other derivatives (C1: 4-NO_2, C2: 4-Br, C3: 4-CF_3). This enhanced activity is likely due to the large, conjugated naphthyl group in C4, which expands the π-electron system and enables stronger π-π interactions with intracellular target proteins. The naphthalene structure also increases lipophilicity, improving membrane permeability and bioavailability, and may enhance binding affinity through stronger interactions with hydrophobic protein regions [58–60]. These features likely contribute to more effective modulation of NF-κB, MAPK, and growth factor signaling pathways involved in cell migration and proliferation. As a result, C4 was identified as the most potent compound for promoting fibroblast proliferation, migration, and anti-inflammatory activity.

Recent research increasingly focuses on reprogramming cellular metabolism rather than treating only the symptoms of diabetes-related complications [61]. In this context, cyanoglycosides derived from Moringa oleifera seeds have been reported to attenuate the progression of diabetic nephropathy by inhibiting the PFKFB3/TGF-β1/SMAD signaling axis, thereby restoring metabolic homeostasis [62]. These findings emphasize that targeting

metabolic dysregulation represents a critical strategy for mitigating diabetes-associated tissue damage. In parallel, the chalcone derivatives evaluated in this study showed strong anti-inflammatory and cytoprotective effects, as well as improved fibroblast function and growth factor signaling. These benefits are likely mediated, at least in part, by modulating cellular stress responses. This suggests that chalcones may help restore redox balance and metabolic integrity in hyperglycemic conditions. Chalcones are naturally occurring flavonoids found in plant sources such as licorice root, apple peel, and various flowers. They are well documented for their anti-inflammatory, antioxidant, and antimelanogenic activities [63]. Several chalcone derivatives disrupt key inflammatory signaling pathways. For example, methyl-1-hydroxy-2-naphthoate suppresses lipopolysaccharide-induced inflammation in macrophages by inhibiting the NFκB, JNK, and p38 MAPK pathways [64]. Similarly, lycochalcone A reduces inflammation by downregulating NFκB activation and prostaglandin E2 (PGE2) production [17]. Consistent with these reports, our findings showed a significant reduction in IL-1β and NFκB expression in diabetic fibroblasts after chalcone treatment (Figs. 4B and 5A and C; $p < 0.05$), supporting the hypothesis that these compounds suppress pro-inflammatory signaling. Additionally, the upregulation of growth factor expression and the increase in total antioxidant status (TAS) indicate that chalcones not only reduce inflammation but also promote cellular repair and strengthen antioxidant defenses. Emerging nanotechnological approaches highlight the need to target inflammation, oxidative stress, and metabolic imbalance in diabetic wound healing [65–67]. Aggregation-induced emission (AIE) luminogen-based nanostructures that release carbon dioxide can accelerate tissue regeneration by suppressing inflammation, reducing oxidative stress, and enabling real-time bioimaging [68]. Similarly, glucose-responsive hydrogels loaded with nanozymes offer a multifunctional platform for regulating local glucose levels, providing antibacterial activity, and supporting tissue repair [69]. The biological effects of chalcone derivatives observed in this study are similar to those achieved with these advanced nanotechnologies. This suggests that chalcones may offer a promising, more accessible therapeutic option for modulating key molecular pathways involved in diabetic tissue repair.

Conclusion

This study comprehensively evaluated the effects of newly synthesized chalcone derivatives on wound healing in a diabetic wound model under high glucose conditions. The results demonstrated that chalcone compounds promoted proliferation and migration in diabetic fibroblasts, suppressed inflammation, and reduced oxidative stress. Inhibition of the NF-κB signaling pathway, reductions in IL-1β and TNF-α levels, and increases in total antioxidant capacity provided evidence for the anti-inflammatory and antioxidant effects of these compounds. Additionally, increased PDGFA expression and higher Ki67 staining intensity indicated enhanced growth factor-mediated tissue repair and cell proliferation. Although chalcone derivatives exhibited relatively low inhibition of α-glucosidase, this effect does not appear to be the primary mechanism in wound healing. The principal effects are mediated through suppression of inflammation, reduction of oxidative stress, and improvement of cellular functions. These findings suggest that chalcones exert a multitarget mechanism of action.

Evaluation of the structure-activity relationship indicates that the higher biological activity of compound C4, which contains a 2-naphthalene ring, compared to other derivatives can be attributed to its extensive π-conjugation, increased lipophilicity, and enhanced capacity to interact with intracellular targets. These properties enable C4 to more effectively suppress cell proliferation, migration, and inflammation. In particular, compound C4 stands out as a promising candidate for further in vivo studies and clinical trials due to its strong biological activity. These results provide a translational basis for developing more effective and versatile strategies for diabetic wound treatment.

Supplementary Information The online version contains supplementary material available at https://doi.org/10.1007/s12010-026-05712-y.

Author contributions **Burcu Demirbağ** (Investigation, Methodology, Writing – Review & Editing), **Hakan Ünver** (Investigation, Methodology, Writing – Review & Editing), **Ayça Kara** (Investigation, Methodology, Writing – Review & Editing), **Adem Necip** (Investigation, Methodology, Writing – Review & Editing), **Metin Yıldırım** (Investigation, Methodology, Funding acquisition, Writing– Review & Editing).

Funding Open access funding provided by the Scientific and Technological Research Council of Türkiye (TÜBİTAK). There is no funding source.

Data Availability The datasets used and/or analyzed during the current study are available from the corresponding author upon reasonable request.

Declarations

Ethical approval Not applicable.

Consent to publish Not applicable.

Consent for publication Not applicable.

AI-assisted tools disclosure The authors declare that ChatGPT (version 5.2, OpenAI) was used exclusively for language editing, grammar correction, and stylistic improvement of the manuscript. The AI tool did not contribute to the study design, data acquisition, data analysis, data interpretation, or the generation of scientific content. All scientific conclusions, interpretations, and responsibility for the work remain solely with the authors.

Clinical trial number Not applicable.

Competing interests The authors declare that they have no conflict of interest.

Open Access This article is licensed under a Creative Commons Attribution 4.0 International License, which permits use, sharing, adaptation, distribution and reproduction in any medium or format, as long as you give appropriate credit to the original author(s) and the source, provide a link to the Creative Commons licence, and indicate if changes were made. The images or other third party material in this article are included in the article's Creative Commons licence, unless indicated otherwise in a credit line to the material. If material is not included in the article's Creative Commons licence and your intended use is not permitted by statutory regulation or exceeds the permitted use, you will need to obtain permission directly from the copyright holder. To view a copy of this licence, visit http://creativecommons.org/licenses/by/4.0/.

References

1. Erukainure, O. L., & Houreld, N. N. (2025). Vanillin enhances photobiomodulation wound healing by modulating glyco-oxidative stress and glucose dysmetabolism in diabetic wounded fibroblast cells. *Journal of Cellular and Molecular Medicine*. https://doi.org/10.1111/jcmm.70537
2. Xie, W., Hu, W., Huang, Z., Li, M., Zhang, H., Huang, X., et al. (2022). Betulinic acid accelerates diabetic wound healing by modulating hyperglycemia-induced oxidative stress, inflammation and glucose intolerance. *Burns & Trauma*. https://doi.org/10.1093/burnst/tkac007
3. Spravchikov, N., Sizyakov, G., Gartsbein, M., Accili, D., Tennenbaum, T., & Wertheimer, E. (2001). Glucose effects on skin keratinocytes. *Diabetes, 50*(7), 1627–1635. https://doi.org/10.2337/diabetes.50.7.1627
4. Kletsas, D., Xuan, Y. H., Huang, B. B., Tian, H. S., Chi, L. S., Duan, Y. M., et al. (2014). High-glucose inhibits human fibroblast cell migration in wound healing via repression of bFGF-regulating JNK phosphorylation. *PLoS ONE*. https://doi.org/10.1371/journal.pone.0108182
5. Kruse, C. R., Singh, M., Sørensen, J. A., Eriksson, E., & Nuutila, K. (2016). The effect of local hyperglycemia on skin cells in vitro and on wound healing in euglycemic rats. *Journal of Surgical Research*, *206*(2), 418–426. https://doi.org/10.1016/j.jss.2016.08.060
6. Al-Rikabi, A. H. A., Tobin, D. J., Riches-Suman, K., & Thornton, M. J. (2021). Dermal fibroblasts cultured from donors with type 2 diabetes mellitus retain an epigenetic memory associated with poor wound healing responses. *Scientific Reports*. https://doi.org/10.1038/s41598-020-80072-z
7. Wang, S., Cheng, W., Wang, X., Wu, Z., & Su, J. (2025). Progress of microneedle targeted modulation technology in the reconstruction of immune microenvironment in diabetic wounds. *European Journal of Medical Research*. https://doi.org/10.1186/s40001-025-02667-4
8. Soheilifar, M. H., Dastan, D., Masoudi-Khoram, N., Keshmiri Neghab, H., Nobari, S., Tabaie, S. M., et al. (2024). In vitro and in vivo evaluation of the diabetic wound healing properties of Saffron (*Crocus sativus* L.) petals. *Scientific Reports*. https://doi.org/10.1038/s41598-024-70010-8
9. Lacina, L., Kolář, M., Pfeiferová, L., Gál, P., & Smetana, K. (2024). Wound healing: Insights into autoimmunity, ageing, and cancer ecosystems through inflammation and IL-6 modulation. *Frontiers in Immunology*. https://doi.org/10.3389/fimmu.2024.1403570
10. Huang, K., Mi, B., Xiong, Y., Fu, Z., Zhou, W., Liu, W., et al. (2025). Angiogenesis during diabetic wound repair: From mechanism to therapy opportunity. *Burns & Trauma*. https://doi.org/10.1093/burnst/tkae052
11. Antidiabetic Effects of Methanolic Extract of Trigonella foenumgraecum Seeds in Diabetic Rats (2023). The Pakistan Veterinary Journal. https://doi.org/10.29261/pakvetj/2023.108
12. Prophylactic Impacts of Lotusine Against Hyperglycaemia (2025). -Induced Oxidative Stress in Hepatic Cells Isolated from Diabetic Rats Via Irs-1/Pi3 K/Akt Pathway. The Pakistan Veterinary Journal. https://doi.org/10.29261/pakvetj/2025.123.
13. Polyphenolic Gum Arabic Extract with Antidiabetic (2025). Antioxidant, Anticancer, and Antimicrobial Activities Enhances Blood Biochemistry, Heat Stress Genes, and Reproductive Hormones in Heat and Cisplatin Nephrotoxicity-Stressed Mice. The Pakistan Veterinary Journal. https://doi.org/10.29261/pakvetj/2025.121
14. ADME studies of TUG. (2022). -770 (a GPR-40 inhibitor agonist) for the treatment of type 2 diabetes using SwissADME predictor: In silico study. *Journal of Applied Pharmaceutical Science*. https://doi.org/10.7324/japs.2022.120418
15. Ishtiaq, F., & Amjad, A. (2025). Nutritional Assessment of Overweight Pregnant Women and its Association with Gestational Diabetes. *Journal of Food Processing & Nutrition Research*, 45–54. https://doi.org/10.22194/fpn.2025.1024
16. Lu, H., Cui, M., Wang, Y., Du, X., Zhou, X., Fang, Y., et al. (2025). Protein-based functional hydrogel improves cutaneous nerve repair and diabetic wound healing. *Nano Research*. https://doi.org/10.26599/nr.2025.94907012
17. Salehi, B., Quispe, C., Chamkhi, I., El Omari, N., Balahbib, A., Sharifi-Rad, J., et al. (2021). Pharmacological properties of chalcones: A review of preclinical including molecular mechanisms and clinical evidence. *Frontiers in Pharmacology*. https://doi.org/10.3389/fphar.2020.592654
18. Wu, J., Li, J., Cai, Y., Pan, Y., Ye, F., Zhang, Y., et al. (2011). Evaluation and discovery of novel synthetic chalcone derivatives as anti-inflammatory agents. *Journal of Medicinal Chemistry, 54*(23), 8110–23. https://doi.org/10.1021/jm200946h
19. Rossi, M., Caruso, F., Crespi, E. J., Pedersen, J. Z., Nakano, G., Duong, M., et al. (2013). Probing antioxidant activity of 2′-hydroxychalcones: Crystal and molecular structures, in vitro antiproliferative studies and in vivo effects on glucose regulation. *Biochimie, 95*(10), 1954–63. https://doi.org/10.1016/j.biochi.2013.07.002

20. Sidharth, S. N., Yuvaraj, A. R., Hui, T. J., Sarojini, B. K., Mashitah, M. Y., & Hegde, G. (2014). Light induced properties of chalcones correlated with molecular structure and photophysical properties for permanent optical storage device. *Advanced Materials Research, 1033–1034*, 1149–53. https://doi.org/10.4028/www.scientific.net/AMR.1033-1034.1149
21. Ansari, F. L., Umbreen, S., Hussain, L., Makhmoor, T., Nawaz, S. A., Lodhi, M. A., et al. (2005). Syntheses and Biological Activities of Chalcone and 1,5-Benzothiazepine Derivatives: Promising New Free-Radical Scavengers, and Esterase, Urease, and?-Glucosidase Inhibitors. *Chemistry & Biodiversity*, *2*(4), 487–496. https://doi.org/10.1002/cbdv.200590029
22. De Spirt, S., Eckers, A., Wehrend, C., Micoogullari, M., Sies, H., Stahl, W., et al. (2016). Interplay between the chalcone cardamonin and selenium in the biosynthesis of Nrf2-regulated antioxidant enzymes in intestinal Caco-2 cells. *Free Radical Biology and Medicine, 91*, 164–71. https://doi.org/10.1016/j.freeradbiomed.2015.12.011
23. Yang, H.-L., Yang, T.-Y., Gowrisankar, Y. V., Liao, C.-H., Liao, J.-W., Huang, P.-J., et al. (2020). Suppression of LPS-induced inflammation by chalcone flavokawain A through activation of Nrf2/ARE-mediated antioxidant genes and inhibition of ROS/NFκB signaling pathways in primary splenocytes. *Oxidative Medicine and Cellular Longevity, 2020*, 1–14. https://doi.org/10.1155/2020/3476212
24. Sökmen, M., & Akram Khan, M. (2016). The antioxidant activity of some curcuminoids and chalcones. *Inflammopharmacology, 24*(2–3), 81–6. https://doi.org/10.1007/s10787-016-0264-5
25. Welday Kahssay, S., Hailu, G. S., & Taye Desta, K. (2021). Design, synthesis, characterization and in vivo antidiabetic activity evaluation of some chalcone derivatives. *Drug Design, Development and Therapy, 15*, 3119–29. https://doi.org/10.2147/dddt.S316185
26. El-Said, K. S., Noser, A. A., & Mohamed, A.-S. (2025). Synthesis of new chalcones and pyrimidine derivatives as antidiabetic agents for type 2 diabetes mellitus: In vitro and in vivo studies. *Bioorganic Chemistry,* Article 163. https://doi.org/10.1016/j.bioorg.2025.108696
27. Martínez-Gutiérrez, A., Bertran, A., Noya, T., Pena-Rodríguez, E., Gómez-Escalante, S., Pascual, S., et al. (2024). New chalcone-derived molecule for the topical regulation of hyperpigmentation and skin aging. *Pharmaceutics*. https://doi.org/10.3390/pharmaceutics16111405
28. Palanisamy, P., Crossia, W. F., Prakash, D., & Antonyraj, A. P. M. (2026). Nanoformulation of stavudine-loaded niosomes: Enhancing drug delivery, entrapment efficiency, and controlled release for improved antiretroviral therapy. *Journal of Orthopaedic Reports*. https://doi.org/10.1016/j.jorep.2025.100677
29. Ma, Z. Y., Qiao, X., Xie, C. Z., Shao, J., Xu, J. Y., Qiang, Z. Y., et al. (2012). Activities of a novel Schiff base copper(II) complex on growth inhibition and apoptosis induction toward MCF-7 human breast cancer cells via mitochondrial pathway. *Journal of Inorganic Biochemistry, 117*, 1–9. https://doi.org/10.1016/j.jinorgbio.2012.08.007
30. Kazkayasi, I., & Denizalti, M. (2023). The effects of metformin and hyaluronic acid on wound healing in high glucose incubated fibroblast cells. *Journal of Research in Pharmacy, 27*(4), 1338–1345. https://doi.org/10.29228/jrp.421
31. Yildirim, M., Kilic, A., Cimentepe, M., Necip, A., & Turedi, S. (2025). Synthesis of bioactive quercetin-boronate esters as a novel biological agent: Enzyme inhibition, anti-microbial properties, computational insights and anti-cancer activity. *Journal of Molecular Structure,* Article 1321. https://doi.org/10.1016/j.molstruc.2024.140216
32. Sarac, B. E., Nissim, L., Karaguzel, D., Arik, G., Kahremany, S., Korshin, E. E., et al. (2025). A novel 2-oxopyrrolidine derivative (LN-53) efficiently induces Nrf-2 signaling pathway activation in human epidermal keratinocytes. *Pharmacological Reports, 77*(5), 1347–63. https://doi.org/10.1007/s43440-025-00757-y
33. Cárdenas-Sandoval, R. P., Bernal-Bernal, L. D., Cabrera-Salazar, S., Gómez-Ramírez, D. M., González-Ballesteros, L. M., Hooker-Mendoza, K. M., et al. (2024). In-vitro study on type I collagen synthesis in low-level laser therapy on the early ligament fibroblasts' healing process. *Lasers in Medical Science*. https://doi.org/10.1007/s10103-024-04151-7
34. Fadilah, N. I. M., Fauzi, M. B., & Maarof, M. (2024). Effect of multiple-cycle collections of conditioned media from different cell sources towards fibroblasts in in vitro wound healing model. *Pharmaceutics*. https://doi.org/10.3390/pharmaceutics16060767
35. Taylor, C. R., & Levenson, R. M. (2006). Quantification of immunohistochemistry—Issues concerning methods, utility and semiquantitative assessment II. *Histopathology, 49*(4), 411–24. https://doi.org/10.1111/j.1365-2559.2006.02513.x
36. Leisibach, P., Schneiter, D., Soltermann, A., Yamada, Y., Weder, W., & Jungraithmayr, W. (2016). Prognostic value of immunohistochemical markers in malignant thymic epithelial tumors. *Journal of Thoracic Disease*, *8*(9), 2580–2591. https://doi.org/10.21037/jtd.2016.08.82

37. Yıldırım, M., Ünver, H., Necip, A., Hord, B., & Ersatir, M. (2026). Novel triphenylphosphonium-hydrazone salts: Integrated experimental and computational insights into AChE inhibition and resistance-overcoming antimicrobial and antibiofilm potential. *Naunyn-Schmiedeberg's Archives of Pharmacology*. https://doi.org/10.1007/s00210-026-05002-8
38. Cimentepe, Ö. Ö., Cimentepe, M., Dogan, K., & Yildirim, M. (2026). Morin-functionalized pHEMA cryogel membranes for combating MDR *Escherichia coli* and MRSA: Antibacterial efficacy and molecular docking study. *Naunyn-Schmiedeberg's Archives of Pharmacology*. https://doi.org/10.1007/s00210-026-04976-9
39. Hussain, S. A., Ghimouz, R., Panda, S. P., Panigrahy, U. P., Marunganathan, V., Shaik, M. R., et al. (2025). Synergistic effects of copper oxide-stigmasterol nanoparticles: A novel therapeutic strategy for oral pathogen biofilms and oral cancer. *Materials Technology*. https://doi.org/10.1080/10667857.2025.2476999
40. Armstrong, D. G., Tan, T.-W., Boulton, A. J. M., & Bus, S. A. (2023). Diabetic foot ulcers. *Jama*. https://doi.org/10.1001/jama.2023.10578
41. Gao, S.-Q., Chang, C., Li, J.-J., Li, Y., Niu, X.-Q., Zhang, D.-P., et al. (2018). Co-delivery of deferoxamine and hydroxysafflor yellow A to accelerate diabetic wound healing via enhanced angiogenesis. *Drug Delivery, 25*(1), 1779–89. https://doi.org/10.1080/10717544.2018.1513608
42. Nayak, S. P. R. R., Haridevamuthu, B., Murugan, R., Dhivya, L. S., Venkatesan, S., Almutairi, M. H., et al. (2024). Furan-based chalcone protects β-cell damage and improves glucose uptake in alloxan-induced zebrafish diabetic model via influencing Peroxisome Proliferator-Activated Receptor agonists (PPAR-γ) signaling. *Process Biochemistry, 142*, 149–61. https://doi.org/10.1016/j.procbio.2024.04.012
43. Adhikari, S., Nath, P., Deb, V. K., Das, N., Banerjee, A., Pathak, S., et al. (2025). Pharmacological potential of natural chalcones: A recent studies and future perspective. *Frontiers in Pharmacology*. https://doi.org/10.3389/fphar.2025.1570385
44. El-Haggar, R., Alsantali, R. I., Aboshanab, A. M., Alkabbani, M. A., Mansour, Y. E., Fatahala, S. S., et al. (2025). Amino acid–modified chalcone derivatives with in vitro and in vivo efficacy against colon cancer. *European Journal of Medicinal Chemistry*. https://doi.org/10.1016/j.ejmech.2025.117963
45. Ma, Z., Ding, Y., Ding, X., Mou, H., Mo, R., & Tan, Q. (2023). PDK4 rescues high-glucose-induced senescent fibroblasts and promotes diabetic wound healing through enhancing glycolysis and regulating YAP and JNK pathway. *Cell Death Discovery*. https://doi.org/10.1038/s41420-023-01725-2
46. Ho, K.-H., Yang, X., Osipovich, A. B., Cabrera, O., Hayashi, M. L., Magnuson, M. A., et al. (2020). Glucose regulates microtubule disassembly and the dose of insulin secretion via tau phosphorylation. *Diabetes, 69*(9), 1936–47. https://doi.org/10.2337/db19-1186
47. Cen, R., Wang, L., He, Y., Yue, C., Tan, Y., Li, L., et al. (2022). Dermal fibroblast migration and proliferation upon wounding or lipopolysaccharide exposure is mediated by Stathmin. *Frontiers in Pharmacology*. https://doi.org/10.3389/fphar.2021.781282
48. Seo, G. Y., Ho, M. T., Bui, N. T., Kim, Y. M., Koh, D., Lim, Y., et al. (2015). Novel naphthochalcone derivative accelerate dermal wound healing through induction of epithelial-mesenchymal transition of keratinocyte. *Journal of Biomedical Science*. https://doi.org/10.1186/s12929-015-0141-3
49. Osmaniye, D., Sağlık, B. N., Khalilova, N., Levent, S., Bayazıt, G., Gül, Ü. D., et al. (2023). Design, synthesis, and biological evaluation studies of novel naphthalene-chalcone hybrids as antimicrobial, anticandidal, anticancer, and VEGFR-2 inhibitors. *ACS Omega, 8*(7), 6669–78. https://doi.org/10.1021/acsomega.2c07256
50. Wang, G., Peng, Z., & Li, Y. (2019). Synthesis, anticancer activity and molecular modeling studies of novel chalcone derivatives containing indole and naphthalene moieties as tubulin polymerization inhibitors. *Chemical and Pharmaceutical Bulletin, 67*(7), 725–728. https://doi.org/10.1248/cpb.c19-00217
51. Avci, H., Gunduz Altintas, H., Yildiz, Y., Coskun, D., & Ari, F. (2023). Effects of chalcone derived compounds on cell cycle and migration capability of human breast and lung cancer cells. *Biology Bulletin, 50*(5), 749–760. https://doi.org/10.1134/s1062359022603159
52. Balachandran, A., Siyumbwa, S. N., Froemming, G. R. A., Beata, M.-M., Małgorzata, J., Lavilla, C. A., et al. (2023). In vitro antioxidant and fibroblast migration activities of fractions eluded from dichloromethane leaf extract of *Marantodes pumilum*. *Life*. https://doi.org/10.3390/life13061409
53. Shi, X., Tang, Y., Sun, X., Liu, Y., Sun, Y., Sun, M., et al. (2016). Interleukin-33-induced immune tolerance is associated with the imbalance of memory and naïve T-lymphocyte subsets. *Molecular Medicine Reports, 14*(5), 4837–43. https://doi.org/10.3892/mmr.2016.5844
54. Behm, B., Babilas, P., Landthaler, M., & Schreml, S. (2011). Cytokines, chemokines and growth factors in wound healing. *Journal of the European Academy of Dermatology and Venereology*, *26*(7), 812–820. https://doi.org/10.1111/j.1468-3083.2011.04415.x

55. Kiritsy, C. P., Antoniades, H. N., Carlson, M. R., Beaulieu, M. T., D'Andrea, M., & Lynch, S. E. (2002). Combination of platelet-derived growth factor-BB and insulin-like growth factor-I is more effective than platelet-derived growth factor-BB alone in stimulating complete healing of full-thickness wounds in "older" diabetic mice. *Wound Repair and Regeneration, 3*(3), 340–50. https://doi.org/10.1046/j.1524-475X.1995.30315.x
56. Pierce, G. F., Tarpley, J. E., Tseng, J., Bready, J., Chang, D., Kenney, W. C., et al. (1995). Detection of platelet-derived growth factor (PDGF)-AA in actively healing human wounds treated with recombinant PDGF-BB and absence of PDGF in chronic nonhealing wounds. *Journal of Clinical Investigation, 96*(3), 1336–50. https://doi.org/10.1172/jci118169
57. Dai, J., Shen, J., Chai, Y., Chen, H., & Martinez, M. P. (2021). IL-1β impaired diabetic wound healing by regulating MMP-2 and MMP-9 through the p38 pathway. *Mediators of Inflammation*. https://doi.org/10.1155/2021/6645766
58. Acosta-Mercado, J., Oliveras-Alsina, A., Marcano-Maiz, A. I., Rivera-Torres, A. P., Cordero-Gimenez, K. T., Malavez-Cajigas, S., et al. (2025). Evaluating naphthalene-modified metallosalen complexes as anticancer agents. *Journal of Medicinal Chemistry, 68*(14), 14300–11. https://doi.org/10.1021/acs.jmedchem.4c03180
59. Chen, Z., Xu, Y., & Qian, X. (2018). Naphthalimides and analogues as antitumor agents: A review on molecular design, bioactivity and mechanism of action. *Chinese Chemical Letters*, *29*(12), 1741–1756. https://doi.org/10.1016/j.cclet.2018.09.020
60. Infield, D. T., Rasouli, A., Galles, G. D., Chipot, C., Tajkhorshid, E., & Ahern, C. A. (2021). Cation-π interactions and their functional roles in membrane proteins. *Journal of Molecular Biology*. https://doi.org/10.1016/j.jmb.2021.167035
61. Dawi, J., Tumanyan, K., Tomas, K., Misakyan, Y., Gargaloyan, A., Gonzalez, E., et al. (2025). Diabetic foot ulcers: Pathophysiology, immune dysregulation, and emerging therapeutic strategies. *Biomedicines*. https://doi.org/10.3390/biomedicines13051076
62. Ge, C., Shi, Z., He, J., Feng, X., Shang, K., Liao, X., et al. (2025). Cyanoglycosides isolated from *Moringa oleifera* seeds inhibited PFKFB3/TGF-β1/smads pathway to alleviate diabetic nephropathy through driving metabolic reprogramming. *Pharmaceutical Biology, 64*(1), 130–42. https://doi.org/10.1080/13880209.2025.2607563
63. Bae, S.-M., & Hyun, C.-G. (2025). Insights on the anti-inflammatory and anti-melanogenic effects of 2′-Hydroxy-2,6′-dimethoxychalcone in RAW 264.7 and B16F10 cells. *Current Issues in Molecular Biology*. https://doi.org/10.3390/cimb47020085
64. Zhang, J.-Y., Jin, H., Wang, G.-F., Yu, P.-J., Wu, S.-Y., Zhu, Z.-G., et al. (2011). Methyl-1-hydroxy-2-naphthoate, a novel naphthol derivative, inhibits lipopolysaccharide-induced inflammatory response in macrophages via suppression of NF-κB, JNK and p38 MAPK pathways. *Inflammation Research, 60*(9), 851–9. https://doi.org/10.1007/s00011-011-0345-2
65. Hussain, R., Hasan, M., Iqbal, K. J., Zafar, A., Tariq, T., Saif, M. S., et al. (2023). Nano-managing silver and zinc as bio-conservational approach against pathogens of the honey bee. *Journal of Biotechnology, 365*, 1–10.
66. Ishaq, R., Zafar, M., Anwar, Z., Dildar, I., Mustafa, G., Tariq, T., et al. (2025). Hyper-production and characterization of exoglucanase through physical, chemical, and combined mutagenesis in Indigenous strain of thermophilic Aspergillus fumigatus. *Applied Biochemistry and Biotechnology*, *197*(6), 4002–4024.
67. Aytar, E. C., Torunoğlu, E. I., Viana, A. R., Düzgün, Z., Piracha, M. H., Flores, E. M. M. (2025). Antioxidant activity, bioavailability and toxicity evaluation, density functional theory, molecular dynamics, and molecular simulation of Neotinea tridentata flower extract. Vegetos.1–14.
68. Tai, Q.-D., Tang, Y., Xie, S.-T., Ye, Y.-Y., Tang, X., Lyu, Q., et al. (2025). Glucose-responsive nanozyme hydrogel for glycemic control and catalytic anti-infective therapy in diabetic wound healing. *Materials Today Bio*. https://doi.org/10.1016/j.mtbio.2025.102405
69. Zhao, M., Huang, J., Yang, H., Yang, R., Guo, S., Liu, Z., et al. (2025). Engineered aggregation-induced emission luminogens-based framework with CO-releasing property for accelerating diabetic wound healing. *Chemical Engineering Journal,* Article 524. https://doi.org/10.1016/j.cej.2025.168981

Publisher's Note Springer Nature remains neutral with regard to jurisdictional claims in published maps and institutional affiliations.

Authors and Affiliations

Burcu Demirbağ[1] · Hakan Ünver[2] · Ayça Kara[3] · Adem Necip[4] · Metin Yıldırım[5]

✉ Metin Yıldırım
metinyildirim4@gmail.com

[1] Health Services Vocational School, Medical Laboratory Techniques Program, Mersin University, Mersin, Türkiye, Turkey

[2] Department of Chemistry, Faculty of Science, Eskisehir Technical University, Eskisehir, Türkiye

[3] Genome and Stem Cell Research Center, Erciyes University, Kayseri, Türkiye, Turkey

[4] Department of Pharmacy Services, Vocational School of Health Services, Harran University, Sanliurfa, Türkiye

[5] Department of Biochemistry, Faculty of Pharmacy, Çukurova University, Adana, Türkiye, Turkey